

## Enantiomerically pure 1,4-benzodiazepine-2,5-diones as Hdm2 antagonists

Juan Jose Marugan,\* Kristi Leonard, Pierre Raboisson, Joan M. Gushue, Raul Calvo, Holly K. Koblish, Jennifer Lattanze, Shuyuan Zhao, Maxwell D. Cummings, Mark R. Player, Carsten Schubert, Anna C. Maroney and Tianbao Lu

*Drug Discovery, Johnson & Johnson Pharmaceutical Research and Development, L.L.C., 665 Stockton Drive, Exton, PA 19341, USA*

Received 14 February 2006; revised 20 March 2006; accepted 20 March 2006  
Available online 21 April 2006

**Abstract**—The 1,4-benzodiazepine-2,5-dione is a suitable template to disrupt the interaction between p53 and Hdm2. The development of an enantioselective synthesis disclosed the stereochemistry of the active enantiomer. An in vitro p53 peptide displacement assay identified active compounds. These activities were confirmed in several cell-based assays including induction of the p53 regulated gene (PIG-3) and caspase activity.  
© 2006 Elsevier Ltd. All rights reserved.

p53 is a nuclear transcription factor that acts as a tumor suppressor. p53 mutations are very common in human tumors, however it remains wild-type in approximately 50% of human cancers.<sup>1</sup> DNA damage due to chemotherapy or radiation increases the levels of p53, promoting the synthesis of proteins involved in DNA repair.<sup>2</sup> As a consequence, elevation of p53 levels assists in cell cycle arrest and/or apoptosis. However, high levels of p53 also leads to increased expression of the human homolog of the double minute-2 protein (Hdm2).<sup>3a</sup> Hdm2 is an E3 ubiquitin ligase and when bound to p53 leads to p53 ubiquitination and degradation by the proteasome complex, thus facilitating resistance to chemotherapy or radiation attack.<sup>3b</sup> It is also known that Hdm2 over-expression is associated with poor clinical outcome for some cancers.<sup>4</sup> Therefore, disruption of the interaction between these two proteins is an appealing target for chemotherapeutic treatment of wild-type p53 tumors.

Several authors have described Hdm2 antagonists.<sup>5</sup> Our group,<sup>6</sup> has published a number of papers describing the

1,4-benzodiazepine-2,5-dione as a suitable template for inhibiting the Hdm2:p53 interaction.

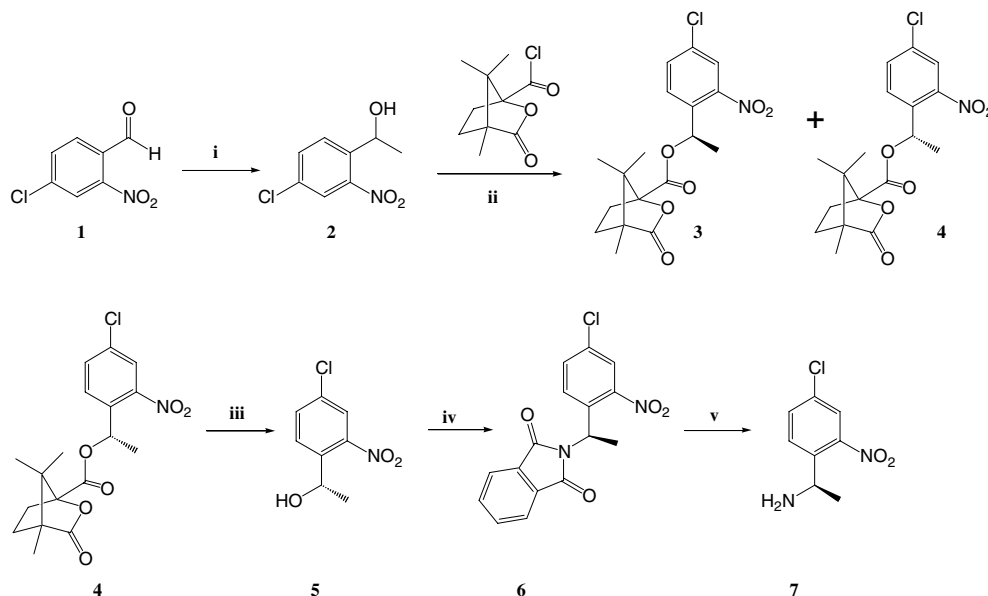
Previously we described the synthesis and SAR of novel racemic 1,4-benzodiazepinediones with improved cellular activity.<sup>6c</sup> Here, we describe the synthesis of enantiomerically pure 1,4-benzodiazepinediones as Hdm2 antagonists, as well as some of the biological activities obtained with these compounds.

In order to evaluate the stereochemical effects on the activity of our inhibitors, we developed a new methodology for the synthesis of enantiomerically pure compounds.

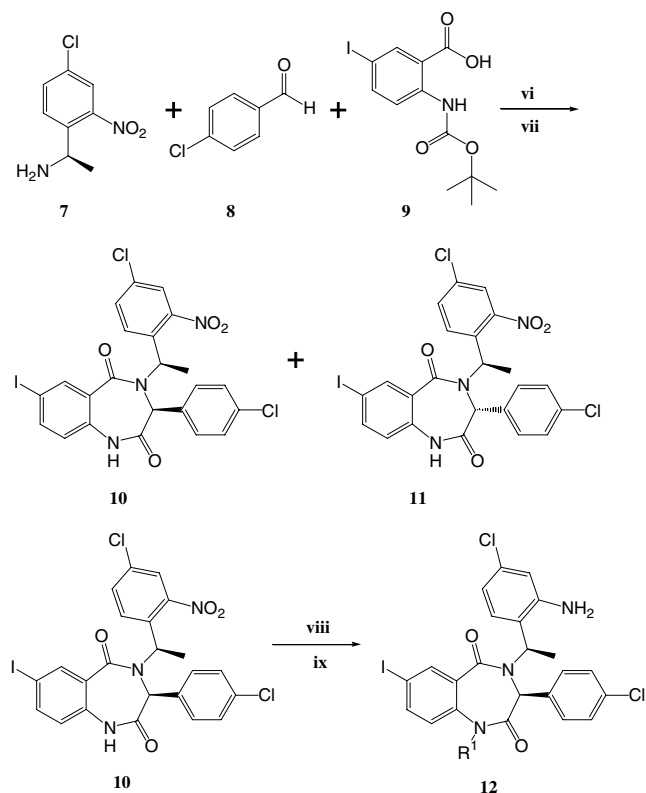
The synthetic strategy, outlined in [Scheme 1](#) and [2](#), consisted of the preparation and selective crystallization of the diastereomeric camphanic esters [3](#) and [4](#). Compound [1](#) was treated with methyl lithium to give the corresponding racemic alcohol [2](#). This was treated with camphanic chloride, followed by selective recrystallization to give [4](#). After separation and hydrolysis, the enantiomerically pure alcohol was transformed to the corresponding amine [7](#) via Mitsunobu reaction with phthalimide and deprotection with hydrazine. In [2](#), amine [7](#) was subjected to an Ugi reaction followed by in situ cyclization to generate a 1:1 mixture of the 1,4-benzodiazepine-2,5-dione templates [10](#) and [11](#),

**Keywords:** Hdm2; Protein–protein interaction; p53.

\* Corresponding author. Tel.: +1 484 888 8257; e-mail addresses: [jmaruga@prdus.jnj.com](mailto:jmaruga@prdus.jnj.com); [Paoyjuan@aol.com](mailto:Paoyjuan@aol.com)



**Scheme 1.** Reagents and conditions: (i) MeLi, THF,  $-78^{\circ}\text{C}$  to rt, 30 min, 73%; (ii) (1S)-(-)-camphanic chloride, NEt<sub>3</sub>, CH<sub>2</sub>Cl<sub>2</sub>, 16 h, 98%; (iii) LiOH, MeOH–H<sub>2</sub>O, 16 h, 93%; (iv) phthalimide, Ph<sub>3</sub>P, DIAD, THF, rt, 3 h, 87%; (v) hydrazine, THF,  $80^{\circ}\text{C}$ , 1 h, 96%.

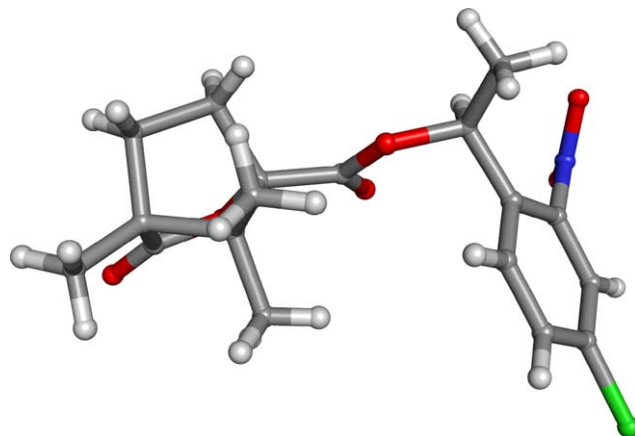


**Scheme 2.** Reagents and conditions: (vi) MeOH, 1-isocyanocyclohexene, rt, 2 days; (vii) AcCl, rt to  $60^{\circ}\text{C}$ , 1 h, 73%; (viii) X-R<sup>1</sup>, Bu<sub>4</sub>NI, K<sub>2</sub>CO<sub>3</sub>, THF,  $80^{\circ}\text{C}$ , 2 h, 40–95%; (ix) NH<sub>4</sub>Cl, Zn(0), AcOH.

which were readily separated by column chromatography. Alkylation of diastereoisomer 10 followed by reduction of the nitro group yielded the target Hdm2 antagonists 12.

The stereochemistry of 12 was assigned on the basis of small molecule X-ray crystallography, conformational analysis and comparison with the structure of a closely related analog bound to Hdm2.<sup>6a</sup>

Small molecule crystallography of compound 4 (Fig. 1), gave an unambiguous assignment of the stereochemistry at the substituted chiral nitrogen.<sup>7</sup> Conformational analysis with the two possible diastereomers at position 3 established a strong preference for one low energy conformer in each case (not shown) Figure 2. Comparison of the preferred conformer for each of the two diastereomers with the published crystal structure of an HDM2-bound analog in this series (Ref. 6a) established that one conformer was essentially identical to that of the close analog bound to HDM2 (Figs. 3 and 4 and additional discussion below) while the other could not fulfill the same binding interactions. On this basis the stereochemistry at position 3 was assigned.



**Figure 1.** X-ray structure determination of compound 4.

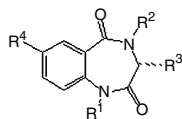


Figure 2.

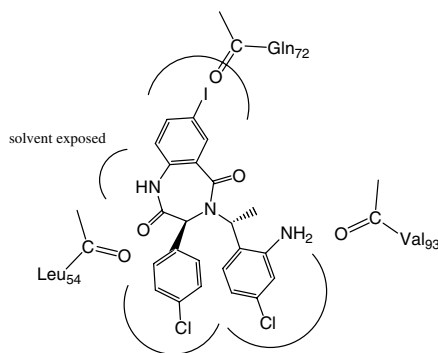


Figure 3. Binding model schematic for the complex of 1,4-benzodiazepine-2,5-diones bound to Hdm2.

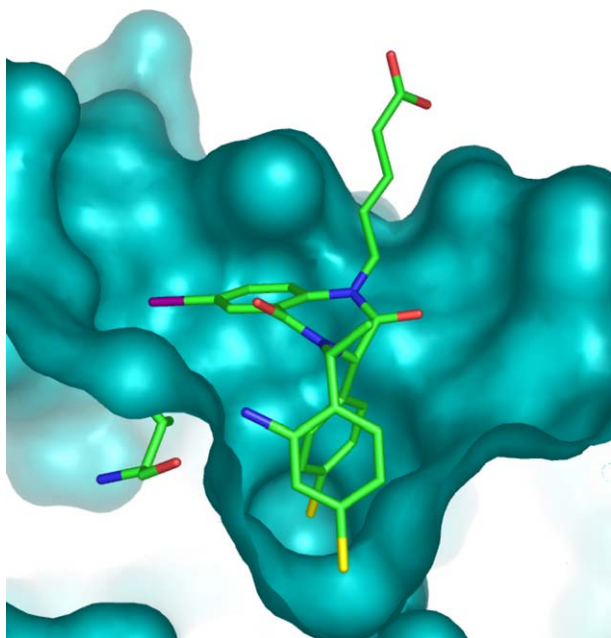


Figure 4. The binding model of the Hdm2-12a complex. In addition to the surface representation of the protein, Val93 is shown in stick form, highlighting the proposed intermolecular hydrogen bond with the aniline N of 12a (see text).

The primary evaluation of the inhibitory activity of final compounds was assessed using a displacement assay of a fluorescent peptide substrate mimicking the sequence of the p53 interaction with Hdm2 (FP assay).<sup>6a</sup> Induction of PIG3 production in JAR carcinoma cells, which are known to overexpress both Hdm2 and p53, was used as secondary screening to confirm that the cellular activity of 12a–m is mediated by p53 activation. The PIG3 production was measured by ELISA.<sup>6d</sup> The results of the FP1 binding assay and the PIG3 production in cell culture are reported in Table 1.

As mentioned in our previous papers,<sup>6b,e</sup> the introduction of an amine functional group in the ortho position of the benzylic ring significantly improved the IC<sub>50</sub> values, but dramatically reduced the cellular activity. The reduction of cellular potency is probably due to the zwitterionic character of the molecule. A binding model of an Hdm2-antagonist complex was used to guide the exploration of solubilizing modifications of this series of molecules.

Based on the previously disclosed structure of a closely related antagonist bound to Hdm2,<sup>6a</sup> we developed a binding model for the complex schematized in Figure 3. The binding interaction involves three lipophilic pockets that are complemented by the three aromatic rings of the bound benzodiazepine. The binding model predicts that the ortho-aniline is well positioned to hydrogen bond with the backbone carbonyl of Val93 (Figs. 3 and 4). This prediction was validated by the observed activity of various ortho-anilines in this series (12e, 12i, and 12k).

The binding model and related crystal structures (not shown) also indicate that the aliphatic acid solubilizing group is relatively solvent-exposed (Fig. 4). We did not expect a strong specificity based on intermolecular binding interactions with substituents at this position.

Analysis of SAR reported in Table 1 shows that the replacement of the valeric acid with the morpholin-4-ylethyl or with 2-(2-methoxyethoxy) ethyl solubilizing chains negatively impacts both the affinity measured in the FP1 binding assay and cellular PIG3 production (compare 12b with 12c and 12g). Different results were observed with the corresponding amino analogues (12a, 12e and 12i), which exhibit approximately the same affinity in the FP1 binding assay. Moreover, the non-acidic compounds 12e and 12i proved to perform better in the PIG3 cell-based assay than the valeroyl derivative 12a. Although the PIG3 production was also increased when the 1-methyl-4-propylpiperazine was used as a solubilizing group (12k), the introduction of 2-morpholin-4-yl-acetamide or 2-piperazin-1-yl-acetamide solubilizing chains (12l and 12m, respectively) was detrimental for the activity. A dramatic difference in activity between the two enantiomers was observed when comparing 12e with 12f and 12g with 12h, where the more active enantiomer was 35 times more potent than the other. Epimerizing of the chiral center of position 3 also decreases the IC<sub>50</sub> value (12c and 12d). The replacement of the iodine substitution of 12e by 1-propynyl moiety afforded 12j, which was found less potent.

Table 2 shows the different activity that some of our most potent compounds have in wild-type versus mutant p53 tumor cell lines. As expected based on the mechanism of action, these compounds showed good selectivity for inhibiting growth of the wild-type p53 MCF7 tumor cell line and a concomitantly reduced activity in the mutant p53 MDA MB 231 cell line.<sup>6d</sup>

Depending upon the p53 activation level, wt-p53 tumor cell lines can be driving toward either a cytostatic

**Table 1.** SAR using FP IC<sub>50</sub> and PIG3 production

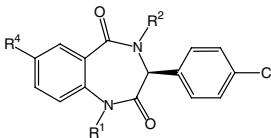
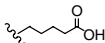
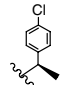
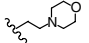
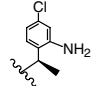
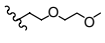
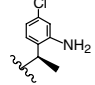
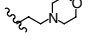
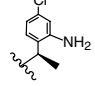

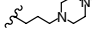
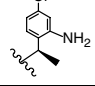
Compound	R <sup>1</sup>	R <sup>2</sup>	R <sup>3</sup>	R <sup>4</sup>	FP IC <sub>50</sub> (μM)	PIG-3		
						1.1 μM	3.3 μM	10 μM
<b>12a<sup>a</sup></b>				I	0.250	47	74	196
<b>12b</b>				I	0.856	60	79.3	208.6
<b>12c</b>				I	2.7	2.8	3.5	23.9
<b>12d</b>				I	6.25	37.3	32.9	36.4
<b>12e</b>				I	0.367	153	683	1404
<b>12f</b>				I	13.1		84.1	103.7
<b>12g</b>				I	2.39	30	58	97
<b>12h</b>				I	>12.5			
<b>12i</b>				I	0.394	96.4	338.1	458.85
<b>12j</b>					0.787	54.8	265.0	474.1
<b>12k</b>				I	0.546	84.0	396.9	412.2
<b>12l</b>				I	5.4	31	32	24
<b>12m</b>				I	1.55	8.6	23.3	33.3

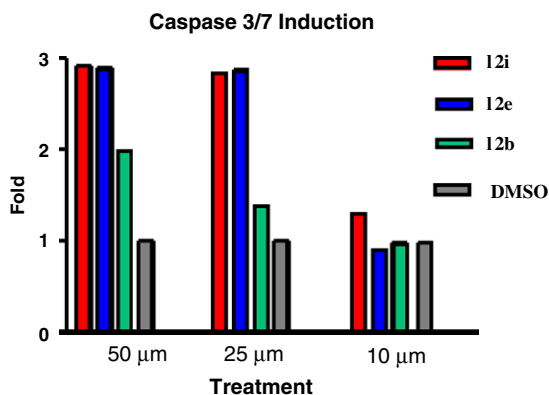
<sup>a</sup> Compound **12a** is the racemic mixture.

or apoptotic event. In order to assess whether these inhibitors can drive the cell toward apoptosis, and therefore anticipate the possible response of our

antagonists on a tumor growth xenograft, we measured the caspase activity in JAR cells. [Figure 5](#) shows the rate of caspase-3 and caspase-7 activation in JAR

**Table 2.** Comparison of the activity of compounds inhibiting growth of wt-p53 tumor cells (MCF7) versus mutant p53 tumor cells (MDA-MB-231)

			BrdU IC <sub>50</sub> (μM)	
	R <sup>1</sup>	R <sup>2</sup>	R <sup>4</sup>	MCF    MDA
<b>12a</b>			I	16    80
<b>12e</b>			I	1.3    10
<b>12i</b>			I	1.1    57
<b>12j</b>				1.7    10
<b>12k</b>			I	0.8    8

**Figure 5.** Caspase induction in JAR cells, 48-h exposure.

cells treated with some of our best antagonists.<sup>8</sup> At 25 and 50 μM, the rate of caspase-3 and -7 production is substantially increased compared to that observed for cells treated with DMSO control. These data clearly indicate that inhibition of the Hdm2 interaction with p53 leads to activation of an apoptotic response in JAR cells.

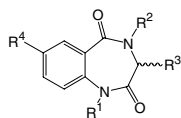
In summary, we have reported herein the synthesis of enantiomerically pure 1,4-benzodiazepine-2,5-diones as Hdm2 antagonists **12a–m** as potent Hdm2 antago-

nists. Structure-base predictions have provided reliable guidance in exploring this class of molecules. Increased potency was obtained by the introduction of an amine functional group in the ortho position of the benzylic ring, leading to the formation of an additional hydrogen bond with Val93. We have also shown that the replacement of the valeric acid side chain with different solubilizing groups has major impact on the cellular potency of this class of molecules. Additionally, these series of compounds induce PIG3 production in cell-based assays, and display selectivity towards wild-type p53 tumor cells. The caspase induction shown with compounds **12i**, **12e**, and **12b** indicates that benzodiazepinediones are capable to activate an apoptotic response in cell-based assay.

### References and notes

- Oren, M. *J. Biol. Chem.* **1999**, *274*, 36031.
- (a) Kubbutat, M. H. G.; Vousden, K. H. *Mol. Med. Today* **1998**, *4*, 250; (b) Harris, C. C. *J. Natl. Cancer Inst.* **1996**, *88*, 1442; (c) Vogelstein, B.; Kinzler, K. W. *Cell* **1992**, *70*, 523.
- (a) Picksley, S. M.; Lane, D. P. *Bioessays* **1993**, *15*, 689; (b) Piette, J.; Nell, H.; Marechal, V. *Oncogene* **1995**, *15*, 1001; (c) Gasco, M.; Crook, T. *Drug Resist. Updat.* **2004**, *6*, 323.
- Momand, J.; Jung, D.; Wilczynski, S.; Niland, J. *Nucleic Acids Res.* **1998**, *26*, 3453.
- (a) Garcia-Echeverria, C.; Chene, P.; Blommers, M. J. J.; Furet, P. *J. Med. Chem.* **2000**, *43*, 3205; (b) Zhao, J.; Wang, M.; Chen, J.; Luo, A.; Wang, X.; Wu, M.; Yin, D.; Liu, Z. *Cancer Lett.* **2002**, *183*, 69; (c) Vassilev, L. T.; Vu, B. T.; Graves, B.; Carvajal, D.; Podlaski, F.; Filipovic, Z.; Kong, N.; Kammlott, U.; Lukacs, C.; Klein, C.; Fotouhi, N.; Liu, E. A. *Science* **2004**, *303*, 844.
- (a) Grasberger, B. L.; Lu, T.; Schubert, C.; Parks, D. J.; Carver, T. E.; Koblisch, H. K.; Cummings, M. D.; LaFrance, L. V.; Milkiewicz, K. L.; Calvo, R. R.; Maguire, D.; Lattanze, J.; Franks, C. F.; Zhao, S.; Ramachandren, K.; Bylebyl, G. R.; Zhang, M.; Manthey, C. L.; Petrella, E. C.; Pantoliano, M. W.; Deckman, I. C.; Spurlino, J. C.; Maroney, A. C.; Tomczuk, B. E.; Molloy, C. J.; Bone, R. F. *J. Med. Chem.* **2005**, *48*, 909; (b) Parks, D. J.; LaFrance, L. V.; Calvo, R. R.; Milkiewicz, K. L.; Gupta, V.; Lattanze, J.; Ramachandren, K.; Carver, T. E.; Petrella, E. C.; Cummings, M. D.; Maguire, D.; Grasberger, B. L.; Lu, T. *Bioorg. Med. Chem. Lett.* **2005**, *15*, 765; (c) Raboisson, P.; Marugan, J. J.; Koblisch, H. K.; Lu, T.; Zhao, S.; Player, M. R.; Maroney, A. C.; Huebert, N. D.; Reed, R. L.; Cummings, M. D. *Bioorg. Med. Chem. Lett.* **2005**, *15*, 1857; (d) Koblisch, H. K.; Zhao, S.; Franks, C. F.; Donatelli, R. R.; LaFrance, L. V.; Leonard, K.; Gushue, J. M.; Parks, D. J.; Calvo, R. R.; Milkiewicz, K. L.; Marugan, J. J.; Raboisson, P.; Cummings, M. D.; Grasberger, B. L.; Lu, T.; Molloy, C. J.; Maroney, A. C. *Mol. Cancer Ther.* **2006**, *5*, 160; (e) Leonard, K.; Marugan, J. J.; Raboisson, P.; Calvo, R.; Gushue, J. M.; Koblisch, H. K.; Lattanze, J.; Zhao, S.; Cummings, M. D.; Player, M. R.; Maroney, A.; Lu, T. *Bioorg. Med. Chem. Lett.*, in press.
- CCDC 601389 contains the supplementary crystallographic data for this paper. These data can be obtained free of charge from The Cambridge Crystallographic Data Centre via [www.ccdc.cam.ac.uk/data\\_request/cif](http://www.ccdc.cam.ac.uk/data_request/cif).

8. Numerical data corresponding to Figure 5:



Compound	R <sub>1</sub>	R <sub>2</sub>	R <sub>3</sub>	R <sub>4</sub>	Fold		
					50 μM	25 μM	10 μM
<b>2</b>				I	1.97	1.37	0.97
<b>5</b>				I	2.89	2.87	0.9
<b>9</b>				I	2.92	2.84	1.29
DMSO					1	1	1